Quaternion-Based Transformation for Extraction of Image-Generating Doppler for ISAR

M. Y. Abdul Gaffar, W. A. J. Nel, and M. R. Inggs

***Abstract*—Inverse synthetic aperture radar (ISAR) is an imaging technique that is dependent on an object's rotational motion over a coherent processing interval. Maritime vessels and aircraft possess 3-D rotational motion, whereas it is only their ISAR contributing motion that is useful to the ISAR imaging process; the contributing motion consists of the Doppler generating axis and the effective angle of rotation. This letter presents a quaternion-based transformation that converts measured attitude and position data into an object's Doppler generating axis and effective angular rotation rate. This transformation is significant since it isolates the component of the motion that directly influences the ISAR image. It provides an alternative approach that can be used to understand the causes of blurring of most ISAR images of sea vessels as well to identify good imaging intervals for applications such as cooperative ISAR for radar cross section measurement purposes.**

***Index Terms*—Cooperative inverse synthetic aperture radar (ISAR), Doppler generating axis of rotation, effective angular rotation rate, optimum imaging intervals, quaternions.**

I. Introduction

INVERSE synthetic aperture radar (ISAR) imaging of maritime vessels has been an active topic of research for the last two decades; much of the research effort in the application of ISAR has focused on classification as shown in papers by Yuan and Casasent [1] and Musman *et al.* [2] In ISAR, the rotational motion of a sea vessel causes scatterers on different parts of the vessel to have different radial velocities with respect to the radar. Consequently, these scatterers can be separated according to their Doppler frequencies, which provide cross-range information.

ISAR imaging of maritime vessels is challenging, since they possess three-dimensional rotational motion: roll, pitch, and yaw. However, it is only a component of this rotational motion that leads to discriminative cross-range information as shown in a paper by Chen and Miceli [3]. In this letter, we define this component of the rotation motion as a vessel's ISAR contributing motion; this can be broken down into the Doppler generating axis and the effective angular rotation rate, which lies in the 2-D plane that is orthogonal to the radar-vessel line of sight vector. These two parameters are important for the ISAR imaging process since the Doppler generating axis of rotation influences the presentation[1] of the vessel in the ISAR image and the effective angular rotation rate affects the resulting cross-range resolution.

Aspects of the time-varying ISAR contributing motion have been formulated in the literature to examine the effect of 3-D motion on the ISAR imaging process. A mathematical expression of the continuously varying Doppler generating axis of rotation can be found in papers by Chen and Miceli [3] and Bao *et al.* [4]. The effect of a time-varying Doppler generating axis of rotation and effective angle of rotation was separately characterized by Abdul Gaffar and Nel [5] and Wong *et al.* [6], respectively. However, the mathematical formulation of the effective angular rotation rate from 3-D motion is lacking in the literature.

This letter proposes a new quaternion-based transformation that calculates the Doppler generating axis of rotation and the effective angular rotation rate from the measured attitude and global positioning system (GPS) position data of an object. These two outputs provide more relevant information for the purpose of ISAR imaging than simply attitude and bearing data themselves. Additionally, the transformation gives the ability of gaining an in-depth understanding of the time-varying nature of these two ISAR related parameters. This understanding can be used to explain the causes of the blurring of most ISAR images of sea vessels that possess 3-D motion. Furthermore, the proposed transformation can be used as an alternative method of identify good imaging intervals with a low degree of 3-D motion for applications such as cooperative ISAR for radar cross section measurement purposes. This is a useful engineering problem since many Navies require their vessels to be measured in order to minimize the effect of scattering hotspots.

II. System Model

We denote a quaternion $\mathbf{q}_x\ (\mathbf{h}, \theta)$ representing a rotation through an angle θ about an axis $\mathbf{h} = [h^1\ h^2\ h^3]$ in vector form as

$$\mathbf{q}_x(\mathbf{h}, \theta) = \left[\cos\left(\frac{\theta}{2}\right) \quad \mathbf{h}\sin\left(\frac{\theta}{2}\right)\right] \tag{1}$$

or in scalar form[2] as

$$\mathbf{q}_x(\mathbf{h}, \theta) = \left[q_x^{\{1\}} \quad q_x^{\{2\}} \quad q_x^{\{3\}} \quad q_x^{\{4\}}\right]. \tag{2}$$

The model considers a vessel with only rotation motion and assumes that any translation motion has been precompensated.

Manuscript received February 29, 2008; revised May 22, 2008, June 9, 2008, and June 13, 2008. Current version published October 22, 2008.

M. Y. Abdul Gaffar and W. A. J. Nel are with the Council for Scientific and Industrial Research, Radar and Electronic Warfare, Pretoria 0001, South Africa.

M. R. Inggs is with the Department of Electrical Engineering, University of Cape Town, Rondebosch 7701, South Africa.

Digital Object Identifier 10.1109/LGRS.2008.2001851

[1]Presentation refers to the orientation of a vessel in an ISAR image [2].

[2]It should be noted that the superscripts $\{1\}$, $\{2\}$, $\{3\}$, and $\{4\}$ are used to denote the respective scalar elements of the quaternion.

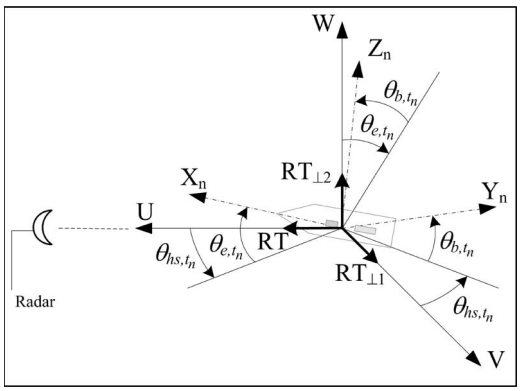

Fig. 1. System model illustrating a vessel's heading-elevation-bank rotation sequence that defines the orientation of the vessel at time t_n.

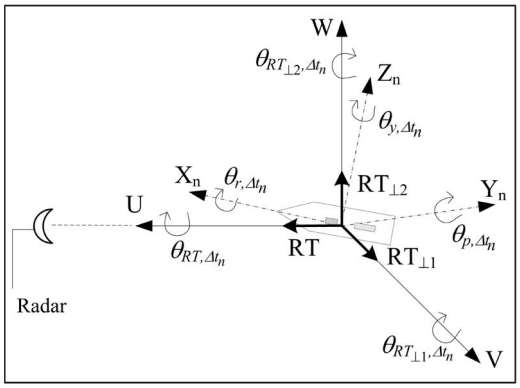

Fig. 2. System model illustrating a vessel's yaw, pitch, and roll angles as well as the effective yaw, pitch, and roll angles with respect to the radar's axes.

Two coordinate axes are defined: the radar coordinate axes (U, V, W) and the vessel's local coordinate axes (X_n, Y_n, Z_n), which rotates when the vessel experiences 3-D rotational motion (see Fig. 1). In the system model, it is assumed that the radar continuously tracks a vessel such that the vessel's center of rotation always lies on the global U.

The system model is defined such that the heading of the vessel is zero when it is sailing directly inbound with respect to the radar; as the vessel rotates clockwise, the heading increases. As a result, the heading used in this system model is given by

$$\theta_{hs,t_n} = \mathrm{mod}(180^\circ + \theta_{h,t_n} - \theta_{br,t_n}, 360^\circ) \tag{3}$$

where $\mathrm{mod}(a, b)$ is the modulus operation of a with b, θ_{br,t_n} denotes the bearing of the vessel obtained from GPS position data, θ_{h,t_n} represents the heading measured from an inertial navigation system (INS), and θ_{hs,t_n} is the heading that is used in the system model, all for time instant t_n. In this letter, the heading, elevation, and pitch angles define the current orientation of the vessel, and the yaw, pitch, and roll angles represent incremental angular motions about a vessel's local axes similar to the convention adopted in [7] (see Figs. 1 and 2).

III. Calculating the Doppler Generating Axis and the Effective Angular Rotation Rate From Measured Data

This section presents the quaternion-based mathematics that is needed to calculate a vessel's ISAR contributing motion from measured attitude and GPS position data. A detailed study of quaternions is presented in a textbook by Kuipers [7].

Let $\mathbf{q}_{\mathrm{tot},\triangle t_n}$ represent the vessel's rotational motion over $\triangle t_n = t_n - t_{n-1}$. If we have two successive motion measurements during time $\triangle t_n$, we can calculate $\mathbf{q}_{\mathrm{tot},\triangle t_n}$ from the attitude measurements using the following formula:

$$\begin{aligned}\mathbf{q}_{\mathrm{tot},\triangle t_n} =& \mathbf{q}_{b,t_{n-1}}(\mathbf{RT}, -\theta_{b,t_{n-1}}) \\ &\otimes \mathbf{q}_{e,t_{n-1}}(\mathbf{RT}_{\perp 1}, -\theta_{e,t_{n-1}}) \\ &\otimes \mathbf{q}_{hs,t_{n-1}}(\mathbf{RT}_{\perp 2}, -\theta_{hs,t_{n-1}}) \\ &\otimes \mathbf{q}_{hs,t_n}(\mathbf{RT}_{\perp 2}, \theta_{hs,t_n}) \\ &\otimes \mathbf{q}_{e,t_n}(\mathbf{RT}_{\perp 1}, \theta_{e,t_n}) \\ &\otimes \mathbf{q}_{b,t_n}(\mathbf{RT}, \theta_{b,t_n})\end{aligned} \tag{4}$$

where $\otimes$ represents quaternion multiplication, bank θ_{b,t_n}, and elevation θ_{e,t_n} angles are measurements from an INS for time t_n, and $\mathbf{RT} = [1\,0\,0]$, $\mathbf{RT}_{\perp 1} = [0\,1\,0]$, $\mathbf{RT}_{\perp 2} = [0\,0\,1]$ are unit vectors about the U, V, W axes, respectively. The calculation of the incremental motion over the time duration $\triangle t_n$ in (4) is accomplished by first reversing the rotation sequence at time t_{n-1} and then applying the rotation sequence at time t_n. The rotation sequence[3] is assumed to be heading, elevation and then bank.

The rotation motion $\mathbf{q}_{\mathrm{tot},\triangle t_n}$ also represents the combined rotation due to the vessel's yaw, pitch, and roll motion, which can be stated mathematically as

$$\begin{aligned}\mathbf{q}_{\mathrm{tot},\triangle t_n} =& \mathbf{q}_{y,\triangle t_n}(\mathbf{z}_{n-1}, \theta_{y,\triangle t_n}) \\ &\otimes \mathbf{q}_{p,\triangle t_n}(\mathbf{y}_{n-1}, \theta_{p,\triangle t_n}) \\ &\otimes \mathbf{q}_{r,\triangle t_n}(\mathbf{x}_{n-1}, \theta_{r,\triangle t_n})\end{aligned} \tag{5}$$

where $\mathbf{x}_n$, $\mathbf{y}_n$, and $\mathbf{z}_n$ are unit vectors about X_n, Y_n, and Z_n, respectively.

However, the vessel's Doppler generating axis of rotation that contributes to the ISAR image lies in the V–W plane since the component of rotation about the U-axis does not provide any Doppler component to the radar. Thus, we need to calculate the effective yaw $\theta_{\mathrm{RT}_{\perp 2},\triangle t_n}$, pitch $\theta_{\mathrm{RT}_{\perp 1},\triangle t_n}$, and roll $\theta_{\mathrm{RT},\triangle t_n}$ rotation angles such that

$$\begin{aligned}\mathbf{q}_{\mathrm{tot},\triangle t_n} =& \mathbf{q}_{\mathrm{ey},\triangle t_n}(\mathbf{RT}_{\perp 2}, \theta_{\mathrm{RT}\perp 2,\triangle t_n}) \\ &\otimes \mathbf{q}_{\mathrm{ep},\triangle t_n}(\mathbf{RT}_{\perp 1}, \theta_{\mathrm{RT}_{\perp 1},\triangle t_n}) \\ &\otimes \mathbf{q}_{\mathrm{er},\triangle t_n}(\mathbf{RT}, \theta_{\mathrm{RT},\triangle t_n}).\end{aligned} \tag{6}$$

The effective yaw, pitch, and roll angles are calculated by the equations found in [7]. Let

$$A_{\triangle t_n} = q^{\{1\}}_{\mathrm{tot},\triangle t_n} q^{\{2\}}_{\mathrm{tot},\triangle t_n} + q^{\{3\}}_{\mathrm{tot},\triangle t_n} q^{\{4\}}_{\mathrm{tot},\triangle t_n} \tag{7}$$

$$B_{\triangle t_n} = -\left(q^{\{1\}}_{\mathrm{tot},\triangle t_n}\right)^2 + \left(q^{\{3\}}_{\mathrm{tot},\triangle t_n}\right)^2 \tag{8}$$

$$D_{\triangle t_n} = \left(q^{\{2\}}_{\mathrm{tot},\triangle t_n}\right)^2 - \left(q^{\{4\}}_{\mathrm{tot},\triangle t_n}\right)^2 \tag{9}$$

then the effective roll angle $\theta_{\mathrm{RT},\triangle t_n}$ about the $\mathbf{RT}$ axis is given by

$$\theta_{\mathrm{RT},\triangle t_n} = \arctan\left(\frac{2A_{\triangle t_n}}{-(B_{\triangle t_n} + D_{\triangle t_n})}\right) \tag{10}$$

[3]This is dependent on the INS being used.

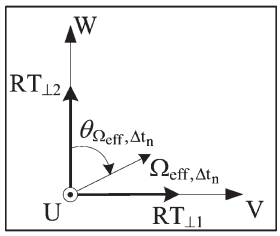

Fig. 3. Illustration of the angle of the Doppler generating axis of rotation.

By defining the following variables

$$\mathbf{q}_{\mathrm{er},\triangle t_n}(\mathbf{RT},\theta_{\mathrm{RT},\triangle t_n}) = \left[\cos\left(\frac{\theta_{\mathrm{RT},\triangle t_n}}{2}\right) \quad \mathbf{RT}\sin\left(\frac{\theta_{\mathrm{RT},\triangle t_n}}{2}\right)\right] \tag{11}$$

$$s_{1,\triangle t_n} = q^{\{1\}}_{\mathrm{tot},\triangle t_n} q^{\{1\}}_{\mathrm{er},\triangle t_n} + q^{\{2\}}_{\mathrm{tot},\triangle t_n} q^{\{2\}}_{\mathrm{er},\triangle t_n} \tag{12}$$

$$s_{2,\triangle t_n} = q^{\{2\}}_{\mathrm{tot},\triangle t_n} q^{\{1\}}_{\mathrm{er},\triangle t_n} - q^{\{1\}}_{\mathrm{tot},\triangle t_n} q^{\{2\}}_{\mathrm{er},\triangle t_n} \tag{13}$$

$$s_{3,\triangle t_n} = q^{\{3\}}_{\mathrm{tot},\triangle t_n} q^{\{1\}}_{\mathrm{er},\triangle t_n} - q^{\{4\}}_{\mathrm{tot},\triangle t_n} q^{\{2\}}_{\mathrm{er},\triangle t_n} \tag{14}$$

$$s_{4,\triangle t_n} = q^{\{4\}}_{\mathrm{tot},\triangle t_n} q^{\{1\}}_{\mathrm{er},\triangle t_n} + q^{\{3\}}_{\mathrm{tot},\triangle t_n} q^{\{2\}}_{\mathrm{er},\triangle t_n} \tag{15}$$

the effective yaw $\theta_{\mathrm{RT}_{\perp 2},\triangle t_n}$ and pitch $\theta_{\mathrm{RT}_{\perp 1},\triangle t_n}$ angles are given by

$$\theta_{\mathrm{RT}_{\perp 2},\triangle t_n} = 2\arctan\left(\frac{s_{4,\triangle t_n}}{s_{1,\triangle t_n}}\right) \tag{16}$$

$$\theta_{\mathrm{RT}_{\perp 1},\triangle t_n} = 2\arctan\left(\frac{s_{3,\triangle t_n}}{s_{1,\triangle t_n}}\right). \tag{17}$$

Consequently, the Doppler generating axis of rotation $\mathbf{\Omega}_{\mathrm{eff},\triangle t_n}$, effective angle of rotation $\theta_{\mathrm{eff},\triangle t_n}$, and the effective angular rotation rate $\dot{\theta}_{\mathrm{eff},\triangle t_n}$ are given by

$$\mathbf{q}_{\mathrm{eff},\triangle t_n}(\Omega_{\mathrm{eff},\triangle t_n},\theta_{\mathrm{eff},\triangle t_n}) = \mathbf{q}_{\mathrm{ey},\triangle t_n}(\mathbf{RT}_{\perp 2},\theta_{\mathrm{RT}_{\perp 2},\triangle t_n}) \otimes \mathbf{q}_{\mathrm{ep},\triangle t_n}(\mathbf{RT}_{\perp 1},\theta_{\mathrm{RT}_{\perp 1},\triangle t_n}) \tag{18}$$

$$\theta_{\mathrm{eff},\triangle t_n} = 2\arccos\left(q^{\{1\}}_{\mathrm{eff},\triangle t_n}\right) \tag{19}$$

$$\dot{\theta}_{\mathrm{eff},\triangle t_n} = \frac{\theta_{\mathrm{eff},\triangle t_n}}{\triangle t_n} \tag{20}$$

$$\mathbf{\Omega}_{\mathrm{eff},\triangle t_n} = \frac{\left[q^{\{2\}}_{\mathrm{eff},\triangle t_n} \quad q^{\{3\}}_{\mathrm{eff},\triangle t_n} \quad q^{\{4\}}_{\mathrm{eff},\triangle t_n}\right]}{\sin\left(\frac{\theta_{\mathrm{eff},\triangle t_n}}{2}\right)} \tag{21}$$

$$\theta_{\Omega_{\mathrm{eff}},\triangle t_n} = \arctan 2\left(q^{\{3\}}_{\mathrm{eff},\triangle t_n}, q^{\{4\}}_{\mathrm{eff},\triangle t_n}\right) \tag{22}$$

where arctan2 is a two-argument function that computes the arctangent of $q^{\{3\}}_{\mathrm{eff},\triangle t_n}/q^{\{4\}}_{\mathrm{eff},\triangle t_n}$ with a range of (–180°, 180°] and $\theta_{\Omega_{\mathrm{eff}},\triangle t_n}$ is the angle of the Doppler generating axis of rotation with respect to the $\mathbf{RT}_{\perp 2}$ axis for the time interval $\triangle t_n$, as shown in Fig. 3.

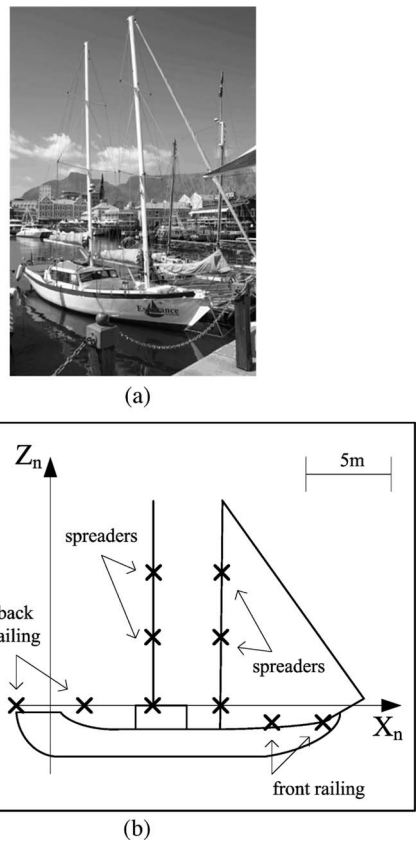

Fig. 4. (a) Photograph of the yacht and (b) point-scatterer model of the yacht.

IV. Results

The proposed transformation was applied to the measured attitude and GPS position data of a yacht, and the results obtained are presented in this section. The motion data were collected using the Thales ADU5 INS/GPS sensor, which has update rates of 5 Hz and 1 Hz for attitude and GPS position data, respectively. The ADU5's heading accuracy was 0.2°; the bank and elevation accuracies were both 0.4°. An experimental X-band radar with a stepped frequency waveform was used to measure the yacht with the following radar parameters: frequency step of 4 MHz, 64 pulses in an ISAR burst, and an effective burst repetition frequency of 154 Hz. A photograph of the yacht that was instrumented and its corresponding point-scatterer model for simulation purposes are shown in Fig. 4. In this model, scatterers were placed at key positions where substantial scattering was expected: metal railings at the back and front of the yacht and at the center of the two spreaders along each mast. The (0, 0, 0) point of Fig. 4(b) corresponds to the placement of the INS onboard the yacht.

Fig. 5 shows the measured motion data corresponding to a data set spanning 2 s. The heading of the vessels confirms the inbound sailing profile of the vessel with an offset of 2° to 4°. The proposed transformation is applied to the data set, and the outputs are shown in Fig. 6; from this diagram, it is clear that both the Doppler generating axis of rotation and the effective angular rotation rate vary with time.

In order to minimize the blurring in an ISAR image, the Doppler generating axis of rotation and the effective angular rotation rate need to be constant [5]. From the data set, we

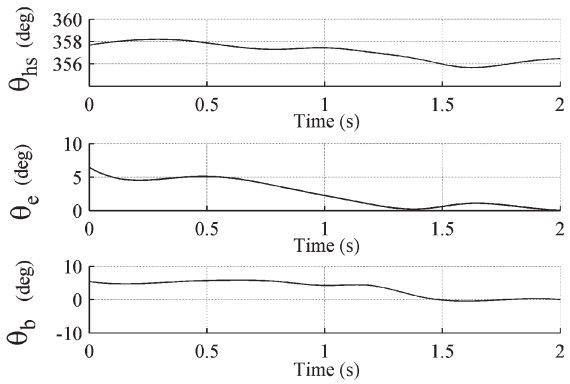

Fig. 5. Measured motion data of a yacht showing its heading, elevation, and bank.

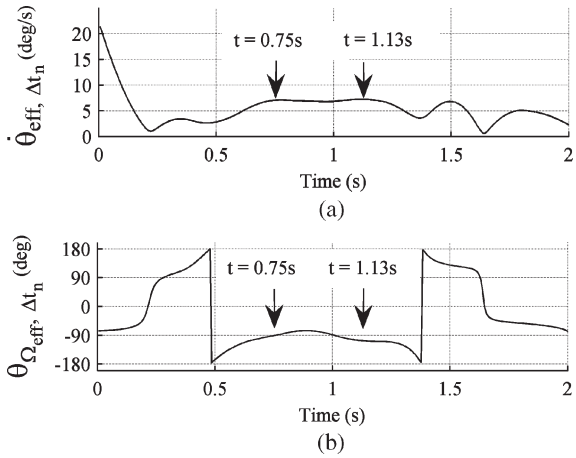

Fig. 6. (a) Effective angular rotation rate and (b) the angle of the Doppler generating axis of rotation.

observe that these two conditions are satisfied during the time interval $0.75\ \text{s} \leq t \leq 1.13\ \text{s}$. Since the Doppler generating axis of rotation is close to -90°, we expect a side-view presentation of the yacht in the ISAR image. This is confirmed by the simulated and measured ISAR images shown in Fig. 7(a) and (b), respectively. The simulated ISAR image was obtained with the point-scatterer model undergoing the motion measured by the INS and radar waveform parameters corresponded to that used in experimental X-band radar. Translation motion compensation in the measured ISAR image was achieved using the global range alignment algorithm in [8] and the autofocus algorithm proposed by Yuan and Casasent [1], which both assume that the vessel has pure 2-D motion. Close agreement between the simulated and the measured ISAR images validates the proposed transformation.

The transformation can also be used to assess the degree of 3-D motion in a coherent processing interval (CPI) for cooperative ISAR applications. This is shown by the measured ISAR images in Fig. 7(b) and (c) for the time intervals $0.75\ \text{s} \leq t \leq 0.88\ \text{s}$ and $1.65\ \text{s} \leq t \leq 1.78\ \text{s}$, respectively. The ISAR

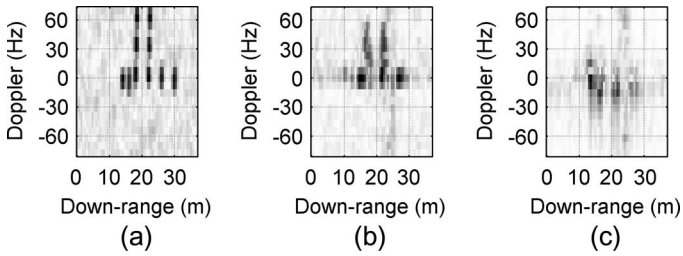

Fig. 7. (a) Simulated ISAR image with measured motion data for CPI of $0.75\ \text{s} \leq t \leq 0.88$ s, (b) measured ISAR image during CPI of $0.75\ \text{s} \leq t \leq 0.88$ s, and (c) measured ISAR image during $1.65\ \text{s} \leq t \leq 1.78$ s.

image in Fig. 7(b) shows a focused image of the yacht with its two masts because the Doppler-generating axis of rotation and the effective angular rotation rate are constant over the CPI. In Fig. 7(c), these two ISAR imaging parameters are varying with time, which leads to an unfocused image since the vessel now has 3-D motion. In this way, suitable imaging intervals that produce focused ISAR images can be separated from poor intervals with 3-D motion that lead to unfocused images.

V. Conclusion

In this letter, a quaternion-based transformation is proposed to convert measured attitude and GPS position data of an object to its Doppler generating axis and effective angular rotation rate. The proposed transformation is important, since it extracts the component of the rotation motion that contributes to the ISAR imaging process. The transformation was applied to measured attitude and GPS position data of a yacht, and the corresponding results were presented. It was shown that this transformation can be used to assess the degree of 3-D motion in a CPI for cooperative ISAR applications.

References

[1] C. Yuan and D. Casasent, "Composite filters for inverse synthetic aperture radar," *Proc. SPIE*, vol. 41, pp. 94–104, Jan. 2002.

[2] S. Musman, D. Kerr, and C. Bachmann, "Automatic recognition of ISAR ship images," *IEEE Trans. Aerosp. Electron. Syst.*, vol. 32, no. 4, pp. 1392–1404, Oct. 1996.

[3] V. C. Chen and W. J. Miceli, "Simulation of ISAR imaging of moving targets," *Proc. Inst. Electr. Eng.—Radar, Sonar Navig.*, vol. 148, no. 3, pp. 160–166, Jun. 2001.

[4] Z. Bao, G. Wang, and L. Luo, "Inverse synthetic aperture radar imaging of maneuvering targets," *Opt. Eng.*, vol. 37, no. 5, pp. 1582–1588, May 1998.

[5] M. Y. Abdul Gaffar and W. A. J. Nel, "Investigating the effect of a target's time-varying Doppler generating axis of rotation on ISAR image distortion," in *Proc. IET Radar Conf.*, session 5b, no. 5, Oct. 2007.

[6] S. Wong, G. Duff, and E. Riseborough, "ISAR image distortion due to small perturbed motion and restoration of distorted images by time–frequency analysis," *Proc. SPIE*, vol. 5102, pp. 200–212, Apr. 2003.

[7] J. Kuipers, *Quaternions and Rotation Sequences: A Primer With Applications to Orbits, Aerospace and Virtual Reality*. Princeton, NJ: Princeton Univ. Press, 1999.

[8] J. Wang and D. Kasilingam, "Global range alignment for ISAR," *IEEE Trans. Aerosp. Electron. Syst.*, vol. 39, no. 1, pp. 351–357, Jan. 2003.